

## Article

# 2D Layer Structure in Two New Cu(II) Crystals: Structural Evolvement and Properties

Jia-Jing Luo<sup>1</sup>, Xiang-Xin Cao<sup>1</sup>, Qi-Wei Chen<sup>1</sup>, Ying Qin<sup>1</sup>, Zhen-Wei Zhang<sup>1,\*</sup> , Lian-Qiang Wei<sup>2,\*</sup> and Qing Chen<sup>1</sup> 

<sup>1</sup> College of Pharmacy, Guangxi Zhuang Yao Medicine Center of Engineering and Technology, Guangxi University of Chinese Medicine, Nanning 530200, China; 15777113797@163.com (J.-J.L.); caoxiangxin@zmc.top (X.-X.C.); cqw77914@163.com (Q.-W.C.); qinying12531@sohu.com (Y.Q.); qing0082@163.com (Q.C.)

<sup>2</sup> College of Chemistry and Bio-Engineering, Hechi University, Hechi 546300, China

\* Correspondence: charliezh@163.com (Z.-W.Z.); wlq259@163.com (L.-Q.W.)

**Abstract:** Two new Cu(II) crystals,  $[\text{Cu}(\text{dtp})\cdot\text{H}_2\text{O}]_n$  (**1**) and  $[\text{Cu}(\text{Hdtp})(\text{bdc})_{0.5}]_n$  (**2**) ( $\text{H}_2\text{dtp} = 4'-(3,5\text{-dicarboxyphenyl})-2,2':6',2'''$ -terpyridine,  $\text{H}_2\text{bdc} = 1,4\text{-benzenedicarboxylic acid}$ ) were synthesized under hydrothermal conditions. X-ray single-crystal structural analysis revealed that the 5-connective Cu(II) is in a distorted tetragonal-pyramidal coordination sphere for both compounds. Crystal **1** shows a “wave-shaped” 2D layer in the structure, while **2** bears a 1D coordination chain structure and a supermolecular 2D layer structure with a thickness of 7.9 Å via 1D chain stacking. PXRD and TGA measurements showed that **1** and **2** are air stable, with thermal stabilities near 300 °C.

**Keywords:** crystals; metal-organic frameworks; Cu(II) ion; 2D layer; structural evolvement



**Citation:** Luo, J.-J.; Cao, X.-X.; Chen, Q.-W.; Qin, Y.; Zhang, Z.-W.; Wei, L.-Q.; Chen, Q. 2D Layer Structure in Two New Cu(II) Crystals: Structural Evolvement and Properties. *Crystals* **2022**, *12*, 585. <https://doi.org/10.3390/cryst12050585>

Academic Editors: Mingyang Chen, Jinbo Ouyang, Dandan Han and Andrey Prokofiev

Received: 6 April 2022

Accepted: 20 April 2022

Published: 22 April 2022

**Publisher's Note:** MDPI stays neutral with regard to jurisdictional claims in published maps and institutional affiliations.



**Copyright:** © 2022 by the authors. Licensee MDPI, Basel, Switzerland. This article is an open access article distributed under the terms and conditions of the Creative Commons Attribution (CC BY) license (<https://creativecommons.org/licenses/by/4.0/>).

## 1. Introduction

In the past few decades, Metal-Organic Framework (MOF) material has been a hot topic in the field of chemistry and materials. It is a kind of hybrid material with a highly ordered network formed by the coordination bond connection between metal ions and organic ligands [1]. It has aroused great interest because of its structural diversity and its wide applications in catalysis [2,3], light-emitting sensors [4–8], gas adsorption/separation [9], magnetism [10], biomedicine [11] and other advanced materials [12]. MOF-based 2D nanosheet materials arouse great interest [13] due to the application of gas separation [14] and molecular sieving membranes [15]. Even though the “top-down” and the “bottom-up” methods have been developed to fabricate this 2D material [16], the understanding of the structure and the consequential tuning of the 2D MOF layer growth are still the key issues at this point.

The 4'-(3,5-dicarboxyphenyl)-2,2':6',2'''-terpyridine ( $\text{H}_2\text{dtp}$ ) ligand is a ditopic near-plane shape linker with *m*-dicarboxylic and tribipyridine groups [17–21], which is a good candidate for the construction of 2D MOFs structures [22]. In order to fulfill the purpose of the 2D layer configuration, it's important to further govern the coordination when a metal ion is coordinated to the tribipyridine group of  $\text{H}_2\text{dtp}$ , as one can expect that a lower coordination number of the metal ion will reduce the possibility of the 3D network extending. Besides six, the coordination number of Cu(II) can be varied to five [23] or four [24], which makes it a potential low-coordinative ion to serve as a node in the linking of the 2D coordination network.

In this paper, two new MOFs with different kinds of 2D structure are synthesized, namely  $[\text{Cu}(\text{dtp})\cdot\text{H}_2\text{O}]_n$  (**1**) and  $[\text{Cu}(\text{Hdtp})(\text{bdc})_{0.5}]_n$  (**2**) ( $\text{H}_2\text{bdc} = 1,4\text{-benzenedicarboxylic acid}$ ). The coordination number of the Cu(II) is five in both compounds. Besides this, **1** shows a “wave-shaped” 2D layer in the structure, as we expected. As for **2**, the introduction of  $\text{bdc}^{2-}$  into the Cu- $\text{H}_2\text{dtp}$  coordination system reduces the 2D network into

the 1D coordination chain; however, a unique supermolecular 2D layer with a thickness of 7.9 Å is also found, which is formed by the orderly array of the 1D chain. A detailed structural analysis shows how the network evolution comes about, and the PXRD and TGA measurements help in understanding the air and thermal stability of the compounds.

## 2. Materials and Methods

### 2.1. Materials and General Methods

The reagents and solvents were commercially available and used as received. All of the other starting materials were of analytical grade, and were used as received, without further purification. The powder X-ray diffraction (PXRD) data were recorded on a Rigaku Miniflex 600 diffractometer (Rigaku, Tokyo, Japan) using Cu K $\alpha$  radiation ( $\lambda = 1.54056$  Å), with a scan speed of  $4^\circ \text{ min}^{-1}$  in the  $2\theta = 5\text{--}45^\circ$  region. Thermogravimetric analyses (TGA) were carried out on a Netzsch STA449 F5 analyzer (Netzsch, Serb, Germany), with the heating of the crystalline samples from room temperature to  $800^\circ\text{C}$  at a rate of  $10^\circ\text{C min}^{-1}$  in a nitrogen atmosphere.

### 2.2. Synthesis of the Complexes

Regarding the synthesis of  $[\text{Cu}(\text{H}_2\text{dtp})]\cdot\text{H}_2\text{O}_n$  (**1**), a mixture of 0.1 mmol  $\text{Cu}(\text{NO}_3)_2\cdot 3\text{H}_2\text{O}$  (0.024 g), 0.05 mmol  $\text{H}_2\text{dtp}$  (0.020 g), 1.3 mL  $\text{H}_2\text{O}$  and 3.6 mL DMA (N, N'-dimethylacetamide), together with 3.6 mL methanol, was sealed in a 15 mL capped vial. The vial was heated at  $150^\circ\text{C}$  for 48 h under autogenous pressure, and then cooled slowly down to room temperature. Light-green crystals with a regular cuboid structure were obtained. The yield was 35% based on  $\text{H}_2\text{dtp}$ . The elemental analysis (%) was calculated for  $\text{C}_{23}\text{H}_{15}\text{CuN}_3\text{O}_5$ : C 57.92 H 3.17 N 8.81; it found: C 57.20 H 3.35 N 8.42. IR ( $\text{cm}^{-1}$ ): 3420 (vs), 1618 (s), 1560 (s), 1443 (s), 1388 (s), 1227 (m), 1178 (m), 1002 (w), 890 (w), 763 (m), 710 (vw), 665 (vw).

Regarding the synthesis of  $[\text{Cu}(\text{H}_2\text{dtp})(\text{bdc})_{0.5}]_n$  (**2**), the synthesis of compound **2** was similar to that of **1**. In addition to using 15 mL  $\text{H}_2\text{O}$  instead of the solvent condition, 0.05 mmol  $\text{H}_2\text{bdc}$  (8 mg) and 0.25 mmol NaOH (10 mg) were added into the system. The mixture was sealed in a 25 mL capped vial, heated at  $140^\circ\text{C}$  for 48 h under autogenous pressure, and then cooled gradually down to room temperature. Similarly, dark-green, slender bulk crystals were obtained. The yield was 32% based on  $\text{H}_2\text{dtp}$ . Elemental analysis (%) was calculated for  $\text{C}_{27}\text{H}_{16}\text{CuN}_3\text{O}_6$ : C 59.83 H 2.98 N 7.75; it found: C 59.20 H 3.25 N 8.01. IR ( $\text{cm}^{-1}$ ): 3444 (vs), 1620 (s), 1554 (s), 1444 (s), 1398 (s), 1250 (m), 1174 (m), 1002 (w), 878 (w), 796 (m), 770 (m), 658 (m).

### 2.3. Crystal Structure Determination

Single crystals of **1** and **2** with the proper dimensions were chosen under an optical microscope and coated with high vacuum grease (Dow Corning Corporation) before being mounted on a glass fiber for the data collection. X-ray crystallography data of **1** and **2** were gathered on a Bruker Apex Smart CCD diffractometer (Bruker, Bremen, Germany) at 293 K with graphite-monochromated Mo K $\alpha$  ( $\lambda = 0.71073$  Å) or Cu K $\alpha$  ( $\lambda = 1.54184$ ) radiation by using the  $\omega$ - $2\theta$  scan mode. The intensity data were corrected for Lorentz and polarization effects (SAINT), and empirical absorption corrections based on equivalent reflections were applied (SADABS) [25]. The structures were solved by direct methods, and were refined by the full-matrix least-squares method on  $F^2$  with the SHELXTL program package [26]. All of the non-hydrogen atoms were refined with anisotropic displacement parameters. The hydrogen atoms were calculated and refined as a riding model. The hydrogen atoms of carboxylic groups and water molecules were located from difference maps. The disordered guest molecules were treated by a solvent mask with the Olex2 program [27]. Crystallographic data for **1** and **2** are given in Table 1. The hydrogen-bonding parameters and selected bond lengths and angles for **1** and **2** are listed in Tables S1–S4 (see Supplementary Materials).

**Table 1.** Crystal data and structure refinement for **1** and **2**.

Compound	1	2
Empirical formula	C <sub>23</sub> H <sub>15</sub> CuN <sub>3</sub> O <sub>5</sub>	C <sub>27</sub> H <sub>16</sub> CuN <sub>3</sub> O <sub>6</sub>
Formula weight	476.92	541.97
Temperature/K	293	293
Crystal system	monoclinic	triclinic
Space group	P2 <sub>1</sub> /n	P1
<i>a</i> /Å	12.3459(3)	8.68340(10)
<i>b</i> /Å	11.0867(3)	11.25970(10)
<i>c</i> /Å	14.8560(4)	11.57420(10)
$\alpha$ /°	90	85.1240(10)
$\beta$ /°	101.181(2)	88.0210(10)
$\gamma$ /°	90	85.7880(10)
Volume/Å <sup>3</sup>	1994.83(8)	1124.042(19)
Z	4	2
$\rho_{\text{calc}}$ g/cm <sup>3</sup>	1.588	1.601
$\mu$ /mm <sup>-1</sup>	1.138	1.824
F(000)	972.0	552.0
Radiation	MoK $\alpha$ ( $\lambda$ = 0.71073)	CuK $\alpha$ ( $\lambda$ = 1.54184)
2 $\theta$ range for data collection/°	3.934 to 59.824	7.67 to 147.946
Index ranges	-16 $\leq$ h $\leq$ 16, -14 $\leq$ k $\leq$ 15, -20 $\leq$ l $\leq$ 20	-10 $\leq$ h $\leq$ 10, -13 $\leq$ k $\leq$ 14, -14 $\leq$ l $\leq$ 13
Reflections collected	28,754	23,945
Independent reflections	5115 [ $R_{\text{int}}$ = 0.0398, $R_{\text{sigma}}$ = 0.0294]	4345 [ $R_{\text{int}}$ = 0.0223, $R_{\text{sigma}}$ = 0.0143]
Data/restraints/parameters	5115/0/292	4345/0/335
Goodness-of-fit on $F^2$	1.078	1.072
Final R indexes [ $I \geq 2\sigma(I)$ ]	$R_1$ = 0.0321, $wR_2$ = 0.0834	$R_1$ = 0.0277, $wR_2$ = 0.0789
Final R indexes [all data]	$R_1$ = 0.0416, $wR_2$ = 0.0871	$R_1$ = 0.0289, $wR_2$ = 0.0800
Largest diff. peak/hole/e Å <sup>-3</sup>	0.33/-0.38	0.25/-0.33

$$R_1 = \frac{\sum ||F_o| - |F_c||}{\sum |F_o|}, wR_2 = \frac{[\sum w(|F_o| - |F_c|)^2 / \sum w|F_o|^2]^{1/2}}{1/2}$$

### 3. Results and Discussion

#### 3.1. Structure Analysis

Uniform single crystals of **1** and **2** were harvested under hydrothermal conditions (Figure 1). Single-crystal X-ray diffraction (SCXRD) analysis revealed that **1** crystallizes in a monoclinic crystal system  $P2_1/n$ . The asymmetrical unit of **1** is composed of fully deprotonating dtp<sup>2-</sup>, one Cu(II) ion, and a guest molecule of H<sub>2</sub>O (Figure 2a). The Cu(II) ion is five-coordinated by nitrogen atoms from pyridine rings and two oxygen atoms from the carboxylic group of neighboring dtp<sup>2-</sup>, forming a distorted tetragonal-pyramidal coordination sphere with the Cu(II)–N and Cu(II)–O bond length in the scale of 1.9463(14)–2.0452(15) Å and 1.9399(12)–2.0950(13) Å, respectively. The coordination properties enable the asymmetry unit of **1** to behave as a four-connective node to link the neighboring units, further forming a “wave-shaped” 2D layer (Figure 2b). The void between the neighboring layers is dotted by the guest water molecules. The two hydrogen atoms of H<sub>2</sub>O form a double H-bond (O–H...O) interaction with the carboxylic groups of neighboring layers with the D–A length of 2.757(2) and 2.880(2) Å [28]. Besides this,  $\pi$ - $\pi$  stacking interactions with a center-center distance of 3.71 and 4.25 Å [29] are also found between the pyridines of dtp<sup>2-</sup> from the neighboring layers (Figure 3). Those intermolecular forces direct the 3D packing of the “wave-shaped” layers in the crystal *b* direction (Figure 2c).

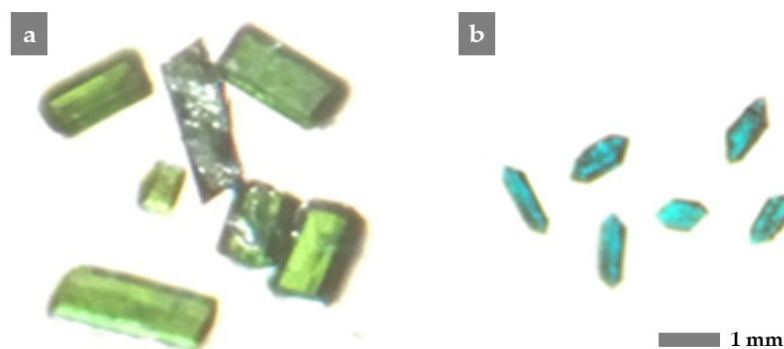


**Figure 1.** The obtained single crystal photos for **1** (a) and **2** (b).

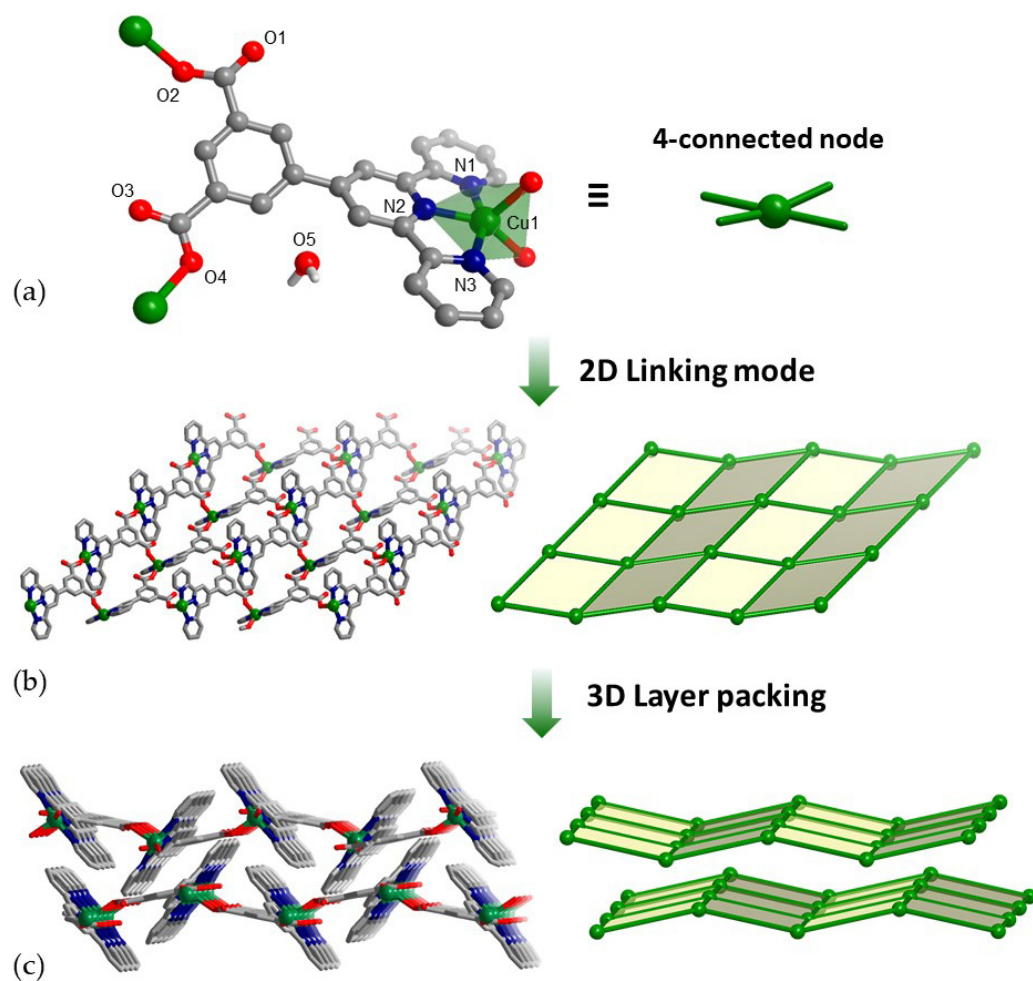


**Figure 2.** Asymmetric unit of **1** (a); the 2D “wave-shaped” layer structure as well as the linking mode of the nodes in **1** (b) and the 3D stacking mode of the layers in **1** (c) (some H atoms are omitted for clarity).

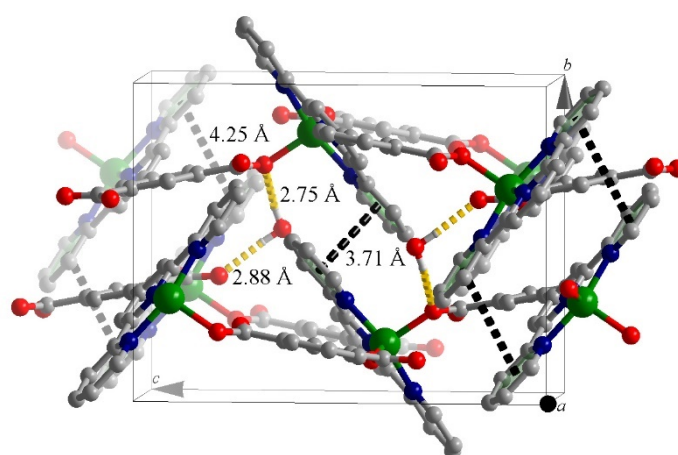


**Figure 3.** H-bond and  $\pi$ - $\pi$  stacking as the interlayer force in **1**.

SCXRD analysis revealed that **2** crystallizes in monoclinic crystal system  $P1$ . The asymmetry unit of **2** is composed of partially deprotonating HdtP<sup>-</sup>, one Cu(II) ion, and half of bdc<sup>2-</sup> (Figure 4a). The Cu(II) ion is five-coordinated by nitrogen atoms from pyridine rings and two oxygen atoms from carboxylic group of bdc<sup>2-</sup> and neighboring HdtP<sup>-</sup>, forming a distorted tetragonal-pyramidal coordination sphere with Cu(II)-N and

Cu(II)-O bond lengths in the scale of 1.9330(13)–2.0217(14) Å and 1.9102(11)–2.2431(13) Å, respectively. The introduction of  $\text{bdc}^-$  into **2** results in a linkage reduction of the asymmetric unit; compared with **1**, the asymmetric unit of **2** behaves as a three-connective node to link the neighboring units, further forming a “ladder-shaped” 1D chain extending in the crystal  $b$  direction (Figure 4b). The 1D chain was found arrayed in the crystal  $a$  direction through the neighboring chain interaction of the H-bond ( $\text{O}-\text{H}\cdots\text{O}$ ) and  $\pi-\pi$  stacking interactions; the former exist between the carboxylic and carboxylate groups with a D-A distance 2.5770(16) Å [28], while the latter is formed between pyridine rings with a center-center distance of 4.38 Å [29]. The inter-chain interactions afford the orderly array of 1D chains, and further give birth to 2D supermolecular layers with a thickness of ca. 7.9 Å (Figure 4c). The final 3D structure of **2** is furnished by the stacking of the 2D supermolecular layers through the neighboring layer interaction of  $\pi-\pi$  stacking within the pyridine rings as well as the benzene rings; the center-center distances are 3.77 and 3.75 Å [29], respectively (Figure 4d).

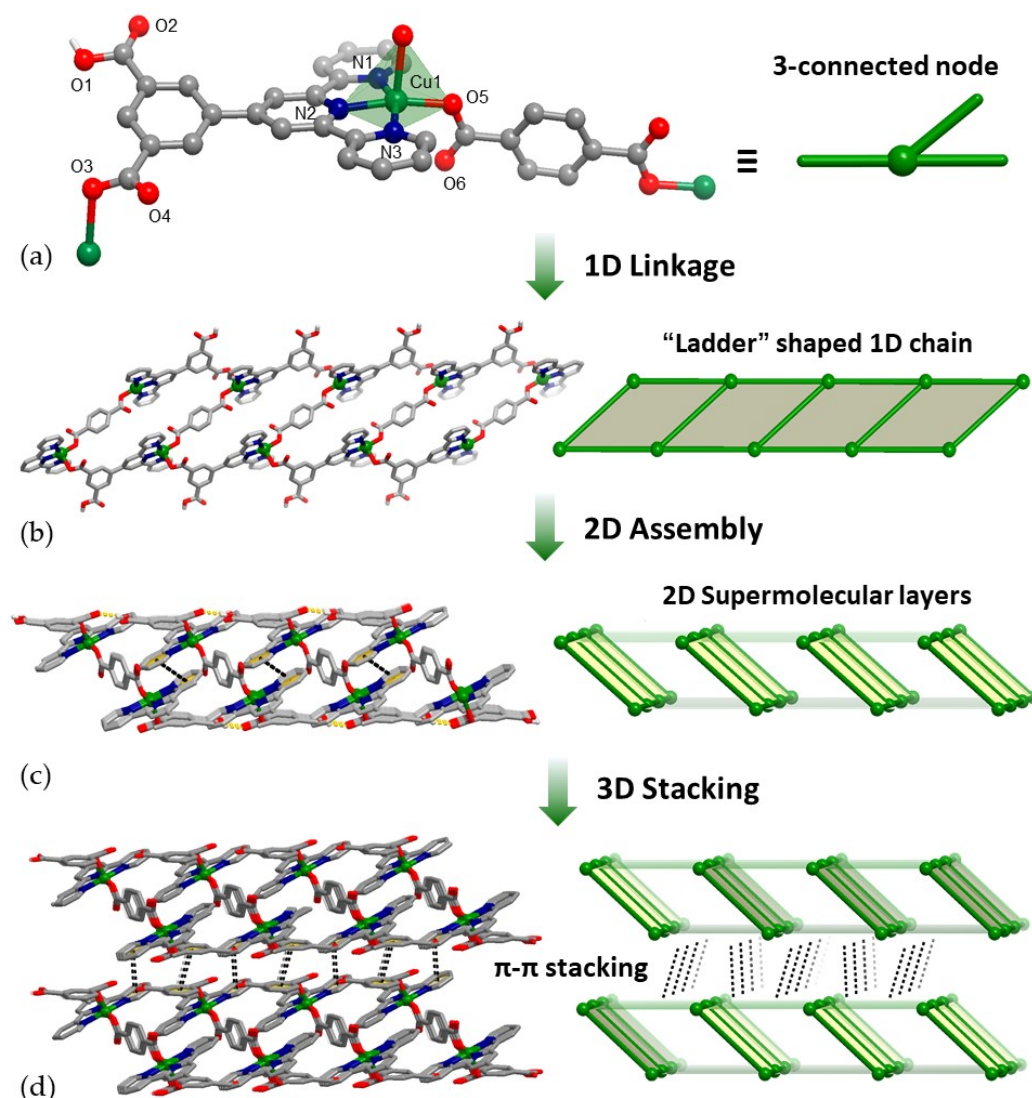


**Figure 4.** Asymmetric unit of **2** (a); the 1D “ladder-shaped” chain structure in **2**, as well as the linking mode of the nodes (b); a 2D supermolecular layer is formed by the orderly array of the 1D chain (c); the 3D structure of **2** (d). Some H atoms are omitted for clarity.

### 3.2. X-ray Diffraction Patterns

The PXRD (powder X-ray diffraction) patterns of complexes **1** and **2** were measured with crystalline samples at room temperature. As is shown in Figure 5, the experimentally determined PXRD patterns and the simulated ones from the SCXRD analyses are in accordance in general, suggesting their phase homogeneity.

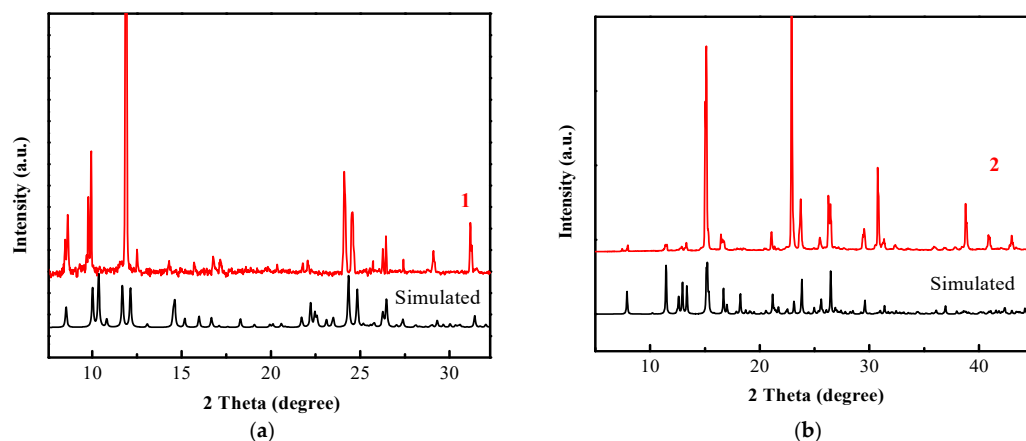


Figure 5. The experimental and simulated PXRD patterns for **1** (a) and **2** (b).

### 3.3. Thermal Analysis

In order to characterize the thermal stability of **1** and **2**, their thermal behaviors were investigated by TGA (Figure 6). For **1**, a weight loss of 9.8% was witnessed in the temperature scale of 25–60 °C, which corresponds to the removal of guest molecules of water. The TG curve goes into a plateau within 160–270 °C, which implies that the framework stability of **1** is up to 270 °C. After that, a weight loss step occurs until 800 °C, which corresponds to the decomposition of organic ligands. (Figure 6a). As for **2**, the first weight loss is 3.6% at 200 °C. Due to the absence of guest molecules according to the SCXRD analysis, the first weight loss was attributed to the elimination of water molecules adhering to the sample's surface. The second weight loss begins at 300 °C; after that, a sharp weight loss occurred, which corresponds to the decomposition of organic ligands. The TGA result of **2** implies that the framework stability of **2** is up to 300 °C (Figure 6b).

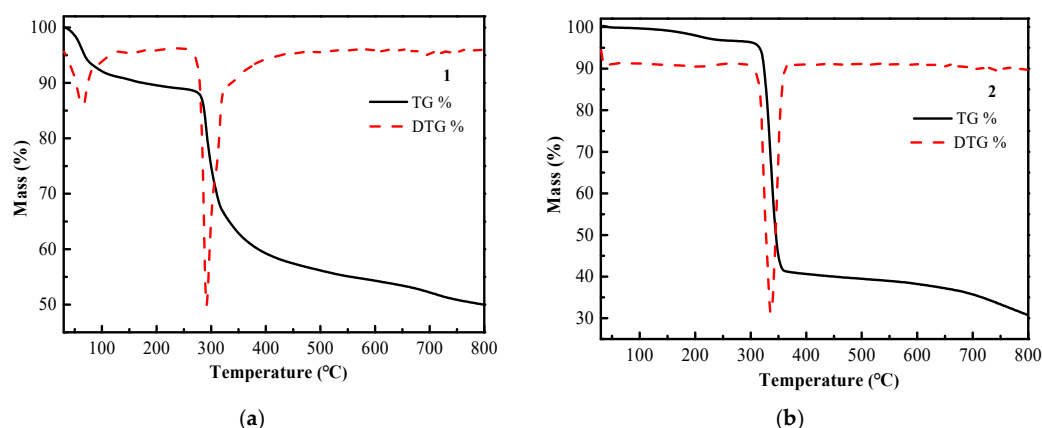


Figure 6. The TGA diagrams for **1** (a) and **2** (b).

## 4. Conclusions

In this work, we presented a structural study of a Cu(II)-H<sub>2</sub>dtp-based MOF system, in which the rational assembly of Cu(II), dtp<sup>2-</sup> or Hdtp<sup>-</sup> as well as auxiliary bdc<sup>2-</sup> linker give birth to two new MOF materials with the formulae of {[Cu(dtp)](H<sub>2</sub>O)<sub>2</sub>]<sub>n</sub> (**1**) and [Cu(Hdtp)(bdc)<sub>0.5</sub>]<sub>n</sub> (**2**). The harvest of 2D “wave-shaped” networks in **1** benefits from the five-coordinative Cu(II), which suggests a low metal ion coordination number in controlling

the formation of the 2D Cu(II)-dtp<sup>2-</sup> network. The introduction of bdc<sup>2-</sup> into the Cu(II)-dtp<sup>2-</sup> system results in a 1D chain structure with a “ladder-shape” in **2**. A unique 2D supermolecular layer with a thickness of 7.9 Å is formed by the orderly array of the 1D chain, which may help to broaden the horizon for the assembly of 2D materials through the intermolecular interactions. The air stability of two MOFs is witnessed by PXRD, and the TGA indicates that the thermal stability of the two MOFs is as high as 300 °C. The unique structure and relatively good stability of these Cu(II)-MOFs inspired us to further isolate the 2D structures of **1** and **2** as 2D materials for further research.

**Supplementary Materials:** The following supporting information can be downloaded at: <https://www.mdpi.com/article/10.3390/cryst12050585/s1>, Table S1: Hydrogen-bonding parameters in **1**; Table S2: Hydrogen-bonding parameters in **2**; Table S3: Selected bond lengths (Å) and angles (°) for **1**; Table S4: Selected bond lengths (Å) and angles (°) for **2**. CCDC 2164393 (**1**) and 2164388 (**2**) contain the supplementary crystallographic data for this paper. These data can be obtained free of charge via [www.ccdc.cam.ac.uk/data\\_request/cif](http://www.ccdc.cam.ac.uk/data_request/cif) (accessed on 5 April 2022), by emailing [data\\_request@ccdc.cam.ac.uk](mailto:data_request@ccdc.cam.ac.uk), or by contacting The Cambridge Crystallographic Data Centre, 12 Union Road, Cambridge CB2 1EZ, U. K.; Fax: +44-1223-336033.

**Author Contributions:** Conceptualization, Z.-W.Z. and L.-Q.W.; methodology, Z.-W.Z., L.-Q.W. and J.-J.L.; validation, J.-J.L., X.-X.C., Q.-W.C. and Y.Q.; formal analysis, J.-J.L., X.-X.C.; Q.-W.C. and Y.Q.; investigation, Z.-W.Z. and L.-Q.W.; resources, Z.-W.Z., L.-Q.W. and J.-J.L.; data curation, J.-J.L.; writing—original draft preparation, Z.-W.Z. and L.-Q.W.; writing—review and editing, Z.-W.Z., L.-Q.W. and Q.C.; visualization, Q.C.; supervision, Z.-W.Z. and L.-Q.W.; project administration, Z.-W.Z. and L.-Q.W.; funding acquisition, Z.-W.Z., L.-Q.W. and J.-J.L. All authors have read and agreed to the published version of the manuscript.

**Funding:** This research was funded by National Natural Science Foundation of China grant number 22161009, Thousands of Young and Middle-aged Backbone Teachers Training Project of Guangxi Colleges and Universities grant number Gui-Jiao 2020-58, University innovation foundation of Guangxi Medicine grant number Gui-Degree 2021 No. 6, Collaborative Innovation Center of Zhuang and Yao Ethnic Medicine grant number 2013 No. 20, Guangxi University of Chinese Medicine Key Project of First-class Discipline Construction grant number 2018XK050, Guangxi Natural Science Foundation grant number 2022GXNSFAA035477.

**Institutional Review Board Statement:** Not applicable.

**Informed Consent Statement:** Not applicable.

**Data Availability Statement:** Not applicable.

**Conflicts of Interest:** The authors declare no conflict of interest.

## References

1. Yin, Z.; Zhou, Y.-L.; Zeng, M.-H.; Kurmoo, M. The Concept of Mixed Organic Ligands in Metal-Organic Frameworks: Design, Tuning and Functions. *Dalton. Trans.* **2015**, *44*, 5258–5275. [[CrossRef](#)] [[PubMed](#)]
2. Wang, Q.; Astruc, D. State of the Art and Prospects in Metal–Organic Framework (MOF)-Based and MOF-Derived Nanocatalysis. *Chem. Rev.* **2020**, *120*, 1438–1511. [[CrossRef](#)] [[PubMed](#)]
3. Yuan, G.; Tan, L.; Wang, P.; Wang, Y.; Wang, C.; Yan, H.; Wang, Y.-Y. MOF-COF Composite Photocatalysts: Design, Synthesis, and Mechanism. *Cryst. Growth Des.* **2022**, *22*, 893–908. [[CrossRef](#)]
4. Shu, Y.; Ye, Q.; Dai, T.; Xu, Q.; Hu, X. Encapsulation of Luminescent Guests to Construct Luminescent Metal–Organic Frameworks for Chemical Sensing. *ACS Sens.* **2021**, *6*, 641–658. [[CrossRef](#)]
5. Hassanein, K.; Cappuccino, C.; Amo-Ochoa, P.; López-Molina, J.; Maini, L.C.; Bandini, E.; Ventura, B. Multifunctional coordination polymers based on copper(I) and mercaptotriacetic ligands: Synthesis, and structural, optical and electrical characterization. *Dalton. Trans.* **2020**, *30*, 10545–10553. [[CrossRef](#)]
6. Rogovoy, M.I.; Berezin, A.S.; Samsonenko, D.G.; Artem'ev, A.V. Silver(I)-organic frameworks showing remarkable thermo-, solvato- and vapochromic phosphorescence as well as reversible solvent-driven 3D-to-0D transformations. *Inorg. Chem.* **2021**, *9*, 6680–6687. [[CrossRef](#)]
7. Artem'ev, A.V.; Davydova, M.P.; Hei, X.-Z.; Rakhmanova, M.I.; Samsonenko, D.G.; Bagryanskaya, I.Y.; Brylev, K.A.; Fedin, V.P.; Chen, J.-S.; Cotlet, M.; et al. Family of robust and strongly luminescent CuI-Based hybrid networks made of ionic and dative bonds. *Chem. Mater.* **2020**, *24*, 10708–10718. [[CrossRef](#)]

8. Troyano, J.; Zapata, E.; Perles, J.; Amo-Ochoa, P.; Fernandez-Moreira, V.; Martínez, J.I.; Zamora, F.; Delgado, S. Multifunctional copper(I) coordination polymers with aromatic mono- and ditopic thioamides. *Inorg. Chem.* **2019**, *5*, 3290–3301. [[CrossRef](#)]
9. Qian, Q.; Asinger, P.A.; Lee, M.J.; Han, G.; Rodriguez, K.M.; Lin, S.; Benedetti, F.M.; Wu, A.X.; Chi, W.S.; Smith, Z.P. MOF-Based Membranes for Gas Separations. *Chem. Rev.* **2020**, *120*, 8161–8266.
10. Zeng, M.-H.; Yin, Z.; Tan, Y.-X.; Zhang, W.-X.; He, Y.-P.; Kurmoo, M. Nanoporous Cobalt(II) MOF Exhibiting Four Magnetic Ground States and Changes in Gas Sorption upon Post-Synthetic Modification. *J. Am. Chem. Soc.* **2014**, *136*, 4680–4688. [[CrossRef](#)]
11. Horcajada, P.; Gref, R.; Baati, T.; Allan, P.K.; Maurin, G.; Couvreur, P.; Férey, G.; Morris, R.E.; Serre, C. Metal–Organic Frameworks in Biomedicine. *Chem. Rev.* **2012**, *112*, 1232–1268. [[CrossRef](#)] [[PubMed](#)]
12. Song, Y.; Fan, R.-Q.; Wang, P.; Wang, X.-M.; Gao, S.; Dua, X.; Yang, Y.-L.; Luan, T.-Z. Copper(I)-iodide based coordination polymers: Bifunctional properties related to thermochromism and PMMA-Doped polymer film materials. *J. Mater. Chem. C* **2015**, *24*, 6249–6259. [[CrossRef](#)]
13. Chakraborty, G.; Park, I.-H.; Medishetty, R.; Vittal, J.J. Two-Dimensional Metal-Organic Framework Materials: Synthesis, Structures, Properties and Applications. *Chem. Rev.* **2021**, *121*, 3751–3891. [[CrossRef](#)] [[PubMed](#)]
14. Rodenas, T.; Luz, I.; Prieto, G.; Seoane, B.; Miro, H.; Corma, A.; Kapteijn, F.; Llabrés i Xamena, F.X.; Gascon, J. Metal–organic framework nanosheets in polymer composite materials for gas separation. *Nat. Mater.* **2015**, *14*, 48–55. [[CrossRef](#)]
15. Peng, Y.; Li, Y.; Ban, Y.; Jin, H.; Jiao, W.; Liu, X.; Yang, W. Metal-organic framework nanosheets as building blocks for molecular sieving membranes. *Science* **2014**, *346*, 1356–1359. [[CrossRef](#)]
16. Duan, J.; Li, Y.; Pan, Y.; Behera, N.; Jin, W. Metal-organic framework nanosheets: An emerging family of multifunctional 2D materials. *Coord. Chem. Rev.* **2019**, *395*, 25–45. [[CrossRef](#)]
17. Wang, H.-H.; Liu, Q.-Y.; Li, L.; Krishna, R.; Wang, Y.-L.; Peng, X.-W.; He, C.-T.; Lin, R.-B.; Chen, B. Nickel-4′-(3,5-dicarboxyphenyl)-2,2′,6′,2′′-terpyridine Framework: Efficient Separation of Ethylene from Acetylene/Ethylene Mixtures with a High Productivity. *Inorg. Chem.* **2018**, *57*, 9489–9494. [[CrossRef](#)]
18. Kang, X.-M.; Wang, W.-M.; Yao, L.-H.; Ren, H.-X.; Zhao, B. Solvent-dependent variations of both structure and catalytic performance in three manganese coordination polymers. *Dalton. Trans.* **2018**, *47*, 6986–6994. [[CrossRef](#)]
19. Kang, X.-M.; Yao, L.-H.; Jiao, Z.-H.; Zhao, B. Two Stable Heterometal-MOFs as Highly Efficient and Recyclable Catalysts in the CO<sub>2</sub> Coupling Reaction with Aziridines. *Chem. Asian J.* **2019**, *14*, 3668–3674. [[CrossRef](#)]
20. Mao, H.-J.; Chen, Q.-X.; Han, B. Two Metal–Organic Coordination Polymers Based on Polypyridyl Ligands: Crystal Structures and Inhibition of Human Spinal Tumour Cells. *Aust. J. Chem.* **2018**, *71*, 902–906. [[CrossRef](#)]
21. Liu, S.-L.; Chen, Q.-W.; Zhang, Z.-W.; Chen, Q.; Wei, L.-Q.; Lin, N. Efficient heterogeneous catalyst of Fe(II)-based coordination complexes for Friedel-Crafts alkylation reaction. *J. Solid. State. Chem.* **2022**, *310*, 123045. [[CrossRef](#)]
22. Bai, N.-N.; Hou, L.; Gao, R.-C.; Liang, J.-Y.; Yang, F.; Wang, Y.-Y. Five 1D to 3D Zn(II)/Mn(II)-CPs based on dicarboxyphenyl-terpyridine ligand: Stepwise adsorptivity and magnetic properties. *Cryst. Eng. Comm.* **2017**, *19*, 4789–4796. [[CrossRef](#)]
23. Massouda, S.S.; Louk, F.R.; David, R.N.; Dartez, M.J.; Nguyn, Q.L.; Labry, N.J.; Fischer, R.C.; Mautner, F.A. Five-coordinate metal(II) complexes based pyrazolyl ligands. *Polyhedron* **2015**, *90*, 258–265. [[CrossRef](#)]
24. Almeida, K.J.d.; Murugan, N.A.; Rinkevicius, Z.; Hugosson, H.W.; Vahtras, O.; Ågren, H.; Cesar, A. Conformations, structural transitions and visible near-infrared absorption spectra of four-, five- and six-coordinated Cu(II) aqua complexes. *Phys. Chem. Chem. Phys.* **2009**, *11*, 508–519. [[CrossRef](#)] [[PubMed](#)]
25. Sheldrick, G.M. *SADABS. Program for Empirical Absorption-Correction of Area Detector Data*; University of Goöttingen: Goöttingen, Germany, 1996.
26. Sheldrick, G.M. SHELXL 2014. *Acta Crystallogr. Sect. C Struct. Chem.* **2015**, *71*, 3–8. [[CrossRef](#)] [[PubMed](#)]
27. Dolomanov, O.V.; Bourhis, L.J.; Gildea, R.J.; Howard, J.A.K.; Puschmann, H. OLEX2: A complete structure solution, refinement and analysis program. *J. Appl. Crystallogr.* **2009**, *14*, 339–341. [[CrossRef](#)]
28. Tiwari, R.K.; Kumar, J.; Behera, J.N. H-bond supported coordination polymers of transition metal sulfites with different dimensionalities. *RSC Adv.* **2015**, *5*, 78389–78395. [[CrossRef](#)]
29. Mishra, B.K.; Sathyamurthy, N.  $\pi$ – $\pi$  Interaction in Pyridine. *J. Phys. Chem. A* **2005**, *109*, 6–8. [[CrossRef](#)]